IEEE Access
Multidisciplinary ⋮ Rapid Review ⋮ Open Access Journal

Received 15 March 2023, accepted 30 March 2023, date of publication 5 April 2023, date of current version 10 April 2023.

Digital Object Identifier 10.1109/ACCESS.2023.3264648

RESEARCH ARTICLE

Analysis of Centimeter and Millimeter-Wave Path Loss at Emergency Exit

MD. ABDUS SAMAD[1], (Member, IEEE), DONG-YOU CHOI[2], (Senior Member, IEEE), HYUNGSEOP SON[1], AND KWONHUE CHOI[1], (Senior Member, IEEE)

[1]Department of Information and Communication Engineering, Yeungnam University, Gyeongsan-si, Gyeongsangbuk-do 38541, South Korea
[2]Department of Information and Communication Engineering, Chosun University, Gwangju 61452, South Korea

Corresponding author: Kwonhue Choi (gonew@yu.ac.kr)

This work was supported by the National Research Foundation of Korea (NRF) Grant funded by the Korean Government [Ministry of Science and ICT (MSIT)] under Grant 2021R1A2C1010370.

ABSTRACT The path loss model for indoor emergency stairs has yet to get enough attention in the literature. Large-scale (LS) path loss models for a stairwell in a 10-stair academic building are the focus of this investigation. We measured the received power with three different links with sophisticated devices and preprocessed it to find the path loss. LS empirical models can be used to determine the path loss in closed environments as the LS models yield the path loss without considering the details of the environmental configurations. Therefore, this study finds LS models—close-in (CI), alpha-beta (AB), and close-in with a frequency-weighted path loss exponent (CIF), alpha-beta-gamma (ABG), when identifying the best LS models from the measured dataset. The parameters of LS models were justified by validating with the previously reported parameters. The path loss exponents extracted from the measured dataset were slightly lower than those reported in the previous investigations. The AB model showed the minimum standard deviations for the three measurement scenarios of the four LS models studied.

INDEX TERMS Emergency stair, path loss modeling, wireless communication, millimeter-wave.

I. INTRODUCTION

Modeling how waves move from the transmitter to the receiver can help plan and manage wireless communication links to provide high-quality network services [1]. Proper radio wave propagation is also needed for good wireless communication facilities for machine-to-machine communication [2], Internet of Things communication [2], and wireless sensor network infrastructure [3]. Many innovative communication techniques, such as high-altitude platform stations [4], low-altitude platform stations [5], unmanned aerial vehicles and unmanned aerial vehicles-assisted communication protocols development got researcher's attention for improvising the outdoor backhaul links that suffer from environmental disturbances or mismatching problems in heterogeneous mediums [6]. Researchers are working on enhancing system components with higher frequency bands [7], with advancements in communication protocols for future communication system advancements. Conversely, the indoor facility-based wave propagation model has garnered attention owing to the ongoing development and necessity of high-quality wireless communication services [8].

The wave can experience a phenomenon known as fading as it travels through the medium it uses to propagate due to facing obstacles both in the outdoor and indoor wireless links. Fading in wave propagation is the variation of the attenuation of a signal, such as rapid changes in signal strength over distance or time interval, varying Doppler shifts on different multipath signals, and time dispersion caused by multipath propagation delays [9]. Generally, fading can be classified into two types—large-scale (LS) and small-scale (SS). The LS propagation techniques show how the environment between the transmitter and receiver affects the average signal attenuation or path loss. The term 'shadowing factor' is linked with the LS technique for indicating how the signal's power at the receiver is dispersed when physical

The associate editor coordinating the review of this manuscript and approving it for publication was Giorgio Montisci.

This work is licensed under a Creative Commons Attribution-NonCommercial-NoDerivatives 4.0 License.
For more information, see https://creativecommons.org/licenses/by-nc-nd/4.0/

barriers are present on the path from the transmitter to the receiver [10]. These variations can be seen on the local-mean powers, which are averages calculated over a short time that remove variations brought on by multipath fading. For SS modeling, on the other hand, instantaneous fluctuations in the strength of the received signal are taken into account instead of the average strength of the signal. In contrast to the 'shadowing factor' in the LS model, the 'mean excess delay' and 'root-mean-square delay spread' are the parameters for determining the effect of multipath fading channels in SS analysis [11].

In the literature [12], [13], path loss and associated parameter modeling techniques are reported. However, a few such methods are tested in emergency stairwell-based measurement experiments. Emergency exits are an essential part of indoor facilities that provide emergency facilities for human lives. An emergency exit or stair is essential for emergency use, but we also use emergency stairwells in our regular activities in a building. Therefore, proper radio wave propagation modeling in a stair environment is essential.

In [14], [15], and [16], image-based ray-tracing techniques were investigated in modeling the wave propagation in a stair environment. A wave propagation model based on a three-dimensional ray-polygon tracing model was proposed, measured at 1.2-to-1.8 GHz on a staircase connecting several floors [17]. In [18], a wave propagation technique was illustrated for stairwell settings using observations made at 900 and 1800 MHz in four stairwells. Further, heuristic diffraction coefficients were used to determine the impact of diffraction from the edges of stairs in [19].

In [20], the fuzzy c-means optimization technique was utilized to determine the cluster. In addition, the Kim-Park indexing algorithm and the multipath component distance were combined to determine the correct number of clusters. On the other hand, several path loss investigations are carried out with the help of LS modeling [21], [22], [23]. In [24], the statistical parameters were extracted from the measured path loss in common type stair using least-square and maximum likelihood estimation techniques. This study suggested a path loss model correlated with transmitter-to-receiver separation distance and antenna height. However, an important parameter, 'frequency,' was not considered for the path loss. In [25], the path loss was found to have a lower slope on the far-end floor than on the near-side floors of the receiver. According to [26], typically, the path loss exponent (PLE) for distinctive indoor and outdoor propagation settings varies from 2 for open spaces to between 3 and 5 for shaded urban cell radios and between 4 and 6 for blocked buildings. In [21], the authors determined LS model's statistical parameters in emergency stairwells at 26, 28, 32, and 38 GHz. They measured path loss with non-line-of-sight (NLOS) links where vertical-polarized signals were transmitted and the receiver received through a vertical-polarized antenna configuration. They also used horn-type antennas at both the transmitter and receiver sites. In [23], the authors determined LS model's statistical parameters in emergency stairs at the 26, 28, 32, and 38 GHz bands in two different stairs. They measured path loss with NLOS and line-of-sight (LOS) links, where signals were sent and received with co-polarization and cross-polarization. They also used horn-type antennas at both the transmitter and receiver sites. In [26], the authors determined CI model's statistical parameters in emergency stairs at 2.4 and 5.8 GHz. They measured path loss with NLOS and LOS links where horizontal-to-horizontal-polarized and vertical-to-vertical-polarized signals were transmitted and received. They also used dipole-dipole antennas both at the transmitter and receiver sites. In [22], the authors determined CI, AB, and CIF model's statistical parameters in emergency stairwells. They measured path loss with NLOS links where co-polarized and cross-polarized signals were transmitted and received. They also used an omnidirectional antenna at the transmitter site and a horn antenna at the receiver site. In [27], the authors determined CI model's statistical parameters in emergency stairs at 26 and 38 GHz. They measured path loss with NLOS links where co-polarized and cross-polarized signals were transmitted and received. In this experiment, horn-type antennas were used both at the transmitter and receiver sites. In [28], the 'Wireless InSite' simulation tool was used to model path loss-related parameters in a staircase environment with a multiple-input multiple-output technique at 60 GHz. Based on the results of that research, the PLE was higher than in other cases that have been reported. The author argued that they validated the higher PLE through simulation in a similar staircase scenario. In [29], the effects of receiver antenna heights were varied from 1-to-1.9 m to observe the impact of antenna height on the received power in stair environments. Based on their research, they found that the path loss and delay spread was significantly reduced when the antenna was placed higher up.

The LS path loss model can yield path loss without considering the detailed shape of the obstruction material. Therefore, the LS model can be helpful in confined spaces, such as an emergency stairwell. The existing 3.7 GHz band (as the 3.5 GHz band was in operation for the 5G network at the time of the measurement, to avoid interference, the 3.7 GHz band has been experimented with) and promising future frequency bands of 28 GHz have been explored for 5G networks in emergency stairwells. Currently, these radio bands are not being investigated for emergency stairs. As a result, this study aids in estimating the power level at the receiver inside the emergency stairwell. This research examined LS path loss modeling on a building's emergency stairwell at Chosun University, South Korea. We used three antenna configurations to measure the 3.7 and 28 GHz bands. The frequency band 3.5 GHz is the operational frequency or expected to use as the carrier frequency shortly for 5G communication in Singapore [30], Nigeria [31], Mexico, India, Colombia, Brazil, Turkey, Morocco, Indonesia, Chile, Malaysia, Pakistan, South Africa, Nigeria, Bangladesh, Egypt, Thailand [32], including South Korea [33]. In addition, in several

measurement-based path loss studies, vertical-to-vertical polarization was deployed to channel sounding [10], [34], [35], [36]. Therefore, we have investigated path loss for horizontal-to-horizontal polarization channels in this study.

In the experimental area of the measurement site, the 3.5 GHz frequency band was in operation. Therefore, we chose 3.7 GHz so that it would not interfere with the 3.5 GHz bands already operational for the 5G network in South Korea and the 28 GHz bands that are likely to be used in the future [33]. We can summarize the highlights of this study as follows.

- Received signal strength was measured up to the tenth floor of an academic building, and the average path losses at each measurement point along the vertical structure were determined. Horn and omnidirectional antennas were used to compare their effects on path loss at 3.7 and 28 GHz bands.
- The measured signal strength was used to determine the path loss to find the optimized statistical parameters of the LS techniques—CI, AB, CIF, and ABG.
- The extracted statistical parameters from the measurement dataset are compared and validated with the reported parameters of the LS models (as available in the literature).

The remaining sections of this study will be structured as follows. The conditions of the experiment and the settings of the hardware used to create the radio channel are described in Section II. This section also introduces the experimental stairs considered in an academic facility used for educational purposes. Section III presents the LS model's mathematical background. Additionally, Section IV presents visual representations of the simulated models generated using the statistical parameters of path losses and measured data. Lastly, the conclusions of this study are arranged in Section V.

II. MEASUREMENT DESCRIPTION AND EQUIPMENT

This section covers the experimental equipment utilized. This description provides the device specifications, a geometric description of the emergency stair, the safety and precaution considered throughout the data acquisition campaign, and the measuring technique. This section ends with discussing how the measured raw data were preprocessed.

A signal generator, suitable power supply units, coaxial cables, omnidirectional antenna, and horn antennas were used to make the measurement channels. In the measurement system, Keysight MXG N5183B was used to generate the signal, and PXI 9393A was used to analyze the signal at the receiver side. This digital signal generator is lighter than most other signal generators. This signal generator can maintain a consistent output power level and prevent overlapping spectra, which might cause interference with another undesired spectrum. The signal generator had a quick adjustment feature and a switching rate of approximately 600 µs. A signal analyzer

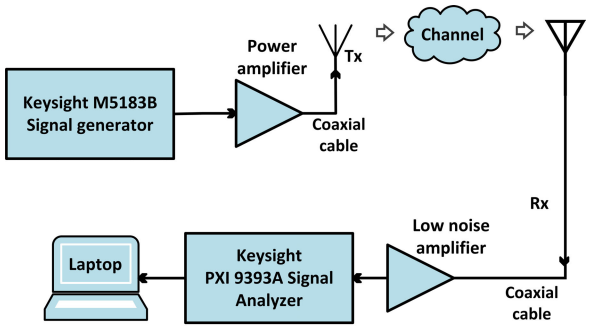

FIGURE 1. Channel sounder architecture. The transmitter and receiver heights were not drawn to scale in this illustration.

covering the frequency range of 3.65 GHz to 50 GHz was used to determine the received power level. Transmitter cable losses at the 3.7 GHz and 28 GHz antennas were 2.8 and 9.4 dB, respectively. In addition, the receiver cable losses at the 3.7- and 28-GHz antennas were 2 dB and 6.2 dB, respectively. Table 1 contains other experiment-related parameters. More details about the used hardware and their specifications are listed in Table 1.

We campaigned for the channel measurement in the 10-storied IT Convergence building of Chosun University (Fig. 2). The transmitter was set on the ground floor, and the receiver system was placed on the 2^{nd}, 3^{rd}, 4^{th}, 5^{th}, 6^{th}, 7^{th}, 8^{th}, 9^{th}, and 10^{th} floor. Table 2 shows the stair structural shape lengths.

The transmitting horn antenna was fixed to a metal tripod and tilted $+15°$ towards the stairs. A coaxial cable connects the signal generator to the transmitting antenna. The antenna for the receiver was also on a metal tripod, but it was not tilted. A more detailed snapshot of the transmitter and receiver is presented in Fig. 4.

The measurement system did not yield path loss data directly. We received the signal strength through the vector signal analyzer in the measurement system. Therefore, we used the gain and attenuation of the transmission cable on both the sender and receiver side to figure out the path loss. All the results were in decibels, so we determined the measured path loss by summing up all the gains and subtracting all the attenuation on the transmission line except the wireless transmission path. Therefore, the path loss (PL) in the wireless transmission link was calculated by (1):

$$\begin{aligned} PL =& (P_{TSL} + P_{TAG} + P_{RAG}) \\ & - (P_{RSL} + P_{TCL} + P_{RCL}) \end{aligned} \tag{1}$$

where P_{TSL} is the transmitted signal strength level, P_{TAG} is the transmitter antenna gain, P_{RAG} is the receiver antenna gain, P_{RSL} is the received signal strength at the receiver side, P_{TCL} is the amount of attenuation in the transmission cable at the transmitter, and P_{RCL} is the amount of attenuation in the transmission cable at the receiver side.

TABLE 1. Specifications of measurement equipment in the measurement campaign. [H=horn antenna, O=omnidirectional antenna].

	3.7 [GHz, HH]	3.7 [GHz, HO]	28 [GHz, HH]
Tx antenna	TAEWA021810	TAEWA021810	WR2820A
Rx antenna	TAEWA021810	TAEODA0467-10	WR2820A
Operational frequency	3.7 GHz	3.7 GHz	28 GHz
Applicable frequency band	2–18 GHz	1–18 GHz	26–40 GHz
Tx height (m)	1.75	1.75	1.75
Rx height (m)	1.5	1.5	1.5
Polarization (Tx)	Horizontal	Horizontal	Horizontal
Polarization (Rx)	Horizontal	Horizontal	Horizontal

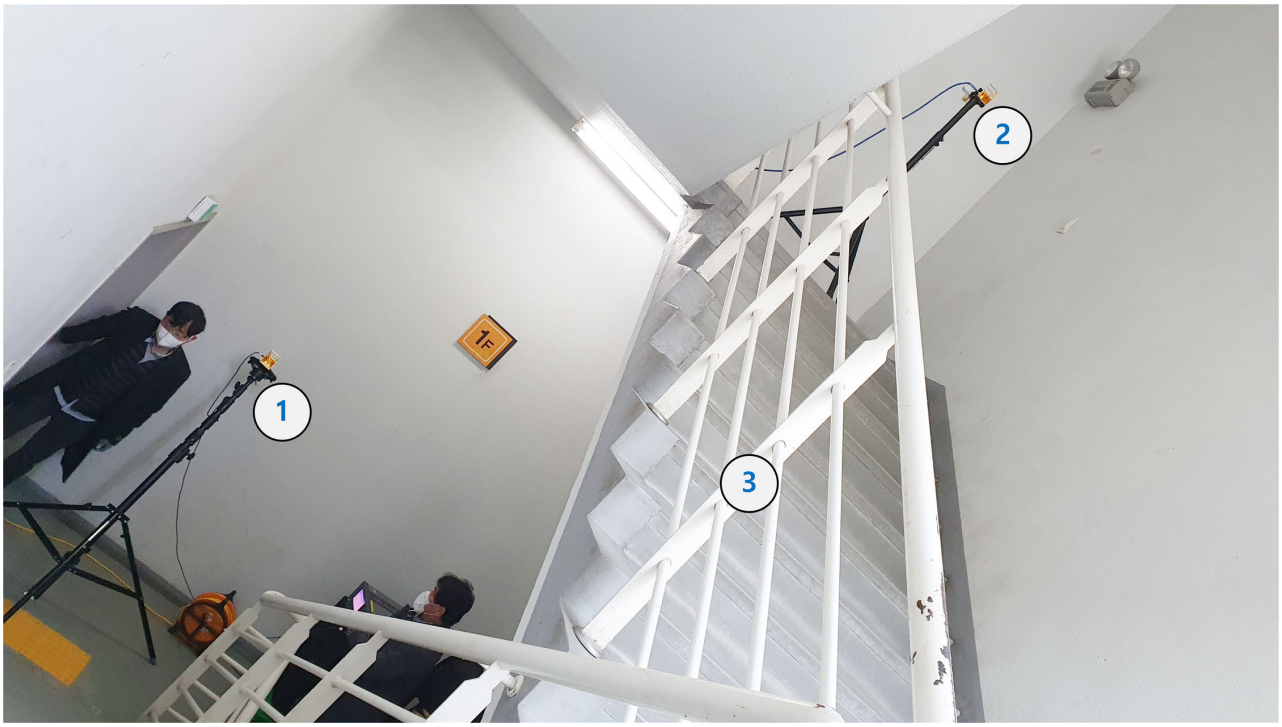

FIGURE 2. A measurement snapshot. In this scenario, the transmitting antenna is placed on the first floor, and the receiving antenna is placed on the second floor. Note: the position of the numbers ①, ②, and ③ respectively, indicates the transmitter, receiver and the metal protection frame of the stair.

III. EMPIRICAL PATH LOSS MODELS

In recent years, various academics and organizations have suggested environment-specific path loss models. As a result, numerous academics have applied the logarithmic distance path loss model to indoor conditions. The formulation of the logarithmic distance path loss model is [37]:

$$\mathrm{PL}(d) = \mathrm{PL}\,(d_0) + 10n\log_{10}\,(d/d_0) + \chi \qquad (2)$$

where n is the PLE, $\mathrm{PL}(d)$ stands for the path loss in decibels at a distance of d from the transmitter, $\mathrm{PL}(d_0)$ stands for the path loss in the reference distance from transmitter d_0, and χ is a Gaussian random variable with a zero-mean and finite standard deviation. The finite standard deviation in the Gaussian distribution represents the amount of 'shadowing' [37]. As mentioned before, 'shadowing' (or 'shadowing factor') is the variation in received signal strength caused by obstacles in the path of signal transmission between the transmitter and the receiver. These changes appear on local-mean powers, which are short-term averages that eliminate changes caused by multipath fading.

Taking into account the effect of frequency on path loss in (2), the following formula can be derived:

$$\mathrm{PL_{CI}}(f, d)[dB] = \mathrm{FSPL}(f, d_0) + 10n\log_{10}(d) + \chi_{\mathrm{CI}} \qquad (3)$$

where $\mathrm{PL_{CI}}$ denotes the path loss in the CI path loss model as a function of distance d and frequency f, and the symbol χ_{CI}

TABLE 2. Stair structural measurement lengths [F=floor].

Floor	Distance (cm)	Floor thickness (cm)
2F	574.5	17
3F	954.8	17
4F	1347.8	17
5F	1611.8	17
6F	1924.9	17
7F	2304.5	17
8F	2705.9	17
9F	3083.8	17
10F	3438.5	17

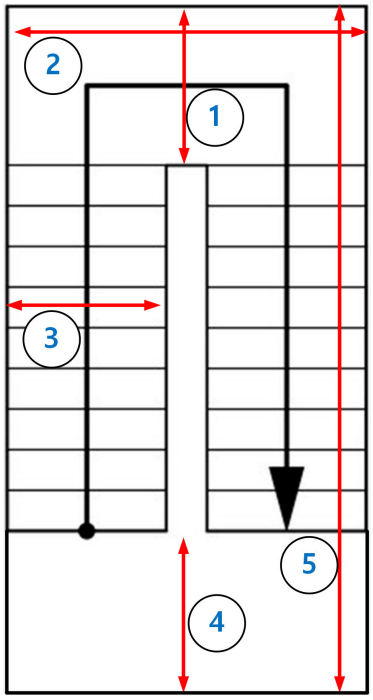

FIGURE 3. The dimension of the measurement site stairwell. In the figure ①=1.583 m, ②=3.468 m, ③=1.591 m, ④=1.583 m, and ⑤=6.694 m.

represents a Gaussian random variable with a zero mean and finite standard deviation.

Furthermore, FSPL(f, d_0) is the projected path loss at d_0 (in m) distance, which analytically can be expressed as $10\log_{10}(\frac{4\pi d_0}{\lambda})^2$, where λ is the carrier frequency wavelength, and n is the PLE. We calculated the optimized PLE and shadowing factor using the procedure described in [38].

The AB path loss model uses a constant, α, as the floating intercept specification, and β is the slope of the path loss when plotting the path loss in the Cartesian coordinate system. We can represent the AB model as [39]:

$$\mathrm{PL}_{\mathrm{AB}}(d)[\mathrm{dB}] = \alpha + 10 \cdot \beta \log_{10}(d) + \chi_{\mathrm{AB}} \quad (4)$$

(a)

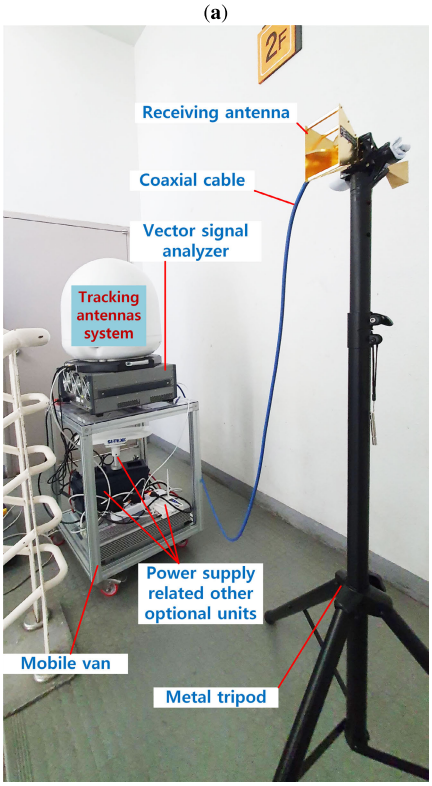

(b)

FIGURE 4. (a) Transmitter and the connected devices, (b) Receiver and the connected devices are shown in the figure. The 'tracking antennas system' shown in the figure was not used for measuring purposes.

where $\mathrm{PL}_{\mathrm{AB}}$ is the path loss depends on the distance parameters d, α stands for the intercepting specification in decibel

scale, β is the gradient of the interpolated line, and χ_{AB} is a Gaussian random variable with a zero mean and finite standard deviation.

Although the parameter FSPL(f, d_0) in (4) appears similar to the parameter α in (3), it is different. The discrepancy is that the parameter FSPL(f, d_0) in the CI model is physically meaningful, whereas the parameter in α is not. Despite their differences, many authors consider these parameters to be the equivalent of FSPL(f, d_0) to α and n to β). Furthermore, authors have compared the parametric statistics of these two models [11].

Therefore, in this study, we considered the intercept parameter (α) to be equivalent to the FSPL and the slope (β) to correspond to the PLE. The optimized values of α, β, and shadow factor were calculated using the procedure described in [38].

The effects of frequency on the path loss were ignored after a reference distance (say, $d_0 = 1$ m) in both the CI and AB models. However, in [35], the CI model was remodeled into the CIF model by recognizing the influence of multiple frequencies on path loss after the reference distance d_0.

With some changes to the original CI model, it is possible to turn the CI model into a CIF model for the multi-frequency operation of the channel. The CI and CIF models use the equal physical relevance of the loss of the FSPL at the radius of the reference distance (for the same reason as in the AB model). As a result, the CIF model can be calculated as follows [35]:

$$\mathrm{PL_{CIF}}(f, d)[\mathrm{dB}] = \mathrm{FSPL}(f, d_0) + \Big(n(1-b) + n \cdot b \cdot (f/f_0)\Big) \cdot 10 \cdot \log(d/d_0) + \chi_{\mathrm{CIF}} \quad (5)$$

where $\mathrm{PL_{CIF}}$ is the path loss conditional on the distance parameters d and frequency f in the CIF model. The term n represents the distance dependency of the PLE, and b is an optimization specification that describes the linear dependence of the path loss on the weighted average of f_0 (in GHz). Furthermore, χ_{CIF} is a Gaussian random variable with zero mean and a finite standard deviation.

ABG is an LS path loss model that can be used for all generic frequencies. However, the model is not appropriate for specific application areas and is only helpful for specific scenarios, such as LOS and NLOS radio links. The path loss, when using the ABG models, can be determined as follows [35]:

$$\mathrm{PL_{ABG}}(d, f)[\mathrm{dB}] = 10\alpha \log_{10}(d) + \beta + 10\gamma \log_{10}(f) + \chi_{\mathrm{ABG}} \quad (6)$$

where $\mathrm{PL_{ABG}}$ denotes the path loss as a function of the distance parameter d and the frequency parameter f, with a reference distance d_0 of 1 m, if the measured distance and frequency are in m and GHz, respectively, the path loss is given in decibels. The letter f represents the operational frequency, whereas the character d represents the three-dimensional Euclidean distance between the transmitter and receiver.

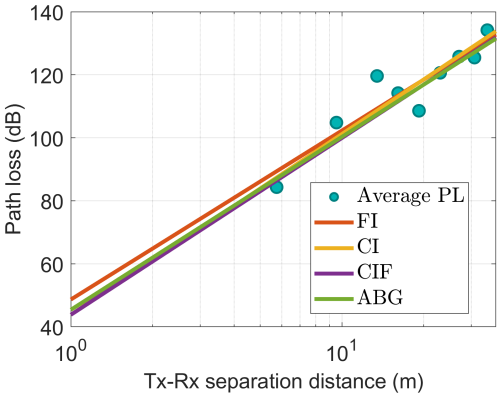

FIGURE 5. Recorded path loss of horn-horn antenna, at 3.7 GHz link simulated with minimum mean square error optimized LS models.

Furthermore, the coefficients α, β, and γ are the statistical parameters of the ABG model. The logarithmic distance and logarithmic frequency coefficients are the parameters α and γ, respectively, and β is the offset parameter adopted to refine the path loss. The random variable χ_{ABG} models the variations of received signal strength at the receiver side. Generally, the noise distribution χ_{ABG} follows a Gaussian distribution with zero-mean and finite variance. The developed weights of the factors α, β, and γ can be figured out by applying the minimum mean square error optimization technique [38]. We used this method to determine the optimized α, β, and γ coefficients on our measured dataset, including distance and path loss at various frequencies.

IV. RESULTS AND DISCUSSIONS

As mentioned, sophisticated tools have been used to measure the strength of the signal received in NLOS situations. This investigation used the LS path loss models CI and AB for single-frequency operation and the CIF and ABG models for multiple-frequency operation. Using various antennas, we set up three distinct types of links at 3.7 GHz (HH), 3.7 GHz (HO), and 28 GHz (HH).

All of the frequency units under consideration were in the GHz band. Consequently, if a frequency measurement unit is lacking, it will likely be in the GHz range. Referring to all considered models, we used a reference distance (d_0) of 1 m. In addition, horizontal polarization was used in the transmitter and the receiver system.

Figures 5, 6, and 7 depict the recorded path losses as matched with the investigated LS models with three different radio links. Figure 5 specifies the calculated path loss at 3.7 GHz with horn-to-horn antenna links simulated using LS models. As we can see, the measured path loss-fitted LS models show almost the same behaviors at the far end, whereas the AB model offers a slightly different behavior at the near end. The PLE of the CI, AB, CIF, and ABG models are 5.48, 5.39, 5.67, and 5.49, respectively. As a result, the AB model offers a lower PLE among these models—a higher PLE results in higher path loss at a higher distance.

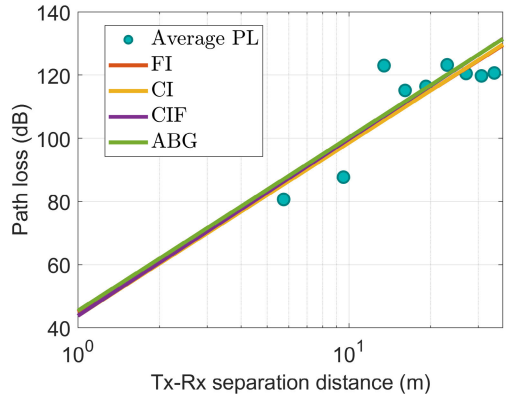

FIGURE 6. Recorded path loss of horn-omnidirectional antenna, at 3.7 GHz link simulated with minimum mean square error optimized LS models.

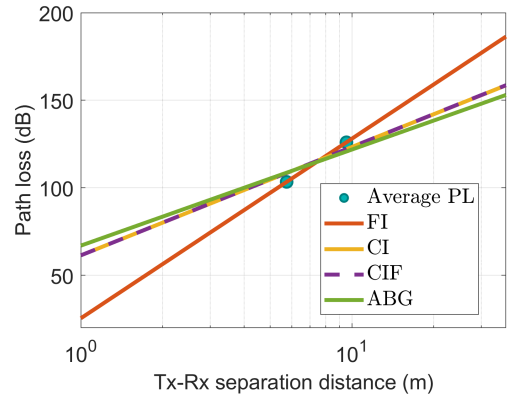

FIGURE 7. Recorded path loss of horn-horn antenna, at 28 GHz link simulated with minimum mean square error optimized LS models.

TABLE 3. Extracted statistical parameters of LS models. [f in GHz, STD=standard deviation of the path loss models].

Coefficients		3.7 [GHz, HH]	3.7 [GHz, HO]	28 [GHz, HH]
FSPL	CI	43.81	43.81	61.38
	AB	44.96	48.65	25.42
	CIF	43.81	43.81	61.38
	ABG		31.48	
PLE	CI	5.48	5.74	6.19
	AB	5.39	5.36	10.26
	CIF		5.67	
	ABG		5.49	
b, γ	b		0.0026	
	γ		2.45	
STD	CI	7.9	5.33	4.52
	AB	7.9	5.25	0
	CIF	8.08	5.57	4.53
	ABG	8.08	5.51	5.26

Figure 6 shows the measured path loss shaped by the LS models with horn-to-omnidirectional antenna links at

TABLE 4. Reported statistical parameters of LS models in the emergency stair. Cells are kept blank if data are unavailable. [f in GHz, V=vertical polarization, H=horizontal polarization, D=direct link/horn antenna, O=omnidirectional antenna, N=NLOS link].

Ref.	Link [f pol.]	PLE			
		CI	AB	CIF	ABG
[26]	2.4 VV	8.88			
	2.4 HH	7.95			
	5.8 VV	11.34			
	5.8 HH	8.13			
[24]		2.25			
[21]	26 VV	7.4	10.9	6.1	9.8
	28 VV	7.9	9.8		
	32 VV	6.6	9.2		
	38 VV	7.1	9.1		
[22]	3.8 VV	2	1.9	1.9	
	28 VV	1.9	1.6	1.9	
[23][a]	26 VV	7.52	10.92	7.44	9.75
	26 HH	7.31			
	26 VH	7.79			
	28 VV	7.6	9.86	7.44	9.75
	28 HH	7.33			
	28 VH	7.86			
	32 VV	7.48	9.17	7.44	9.75
	32 HH	7.6			
	32 VH	7.96			
	38 VV	7.36	9.09	7.44	9.75
	38 HH	7.26			
	38 VH	7.57			
[23][b]	26 VV	7.52	10.92	7.44	9.75
	26 HH	7.31			
	26 VH	7.79			
	28 VV	7.6	9.86	7.44	9.75
	28 HH	7.33			
	28 VH	7.86			
	32 VV	7.48	9.17	7.44	9.75
	32 HH	7.6			
	32 VH	7.96			
	38 VV	7.36	9.09	7.44	9.75
	38 HH	7.26			
	38 VH	7.57			
[27]	26 VV, [D,N]	4.18			
	26 VH [D,N]	4.46			
	38 VV [D,N]	3.97			
	38 VH [D,N]	4			
	26 VV [O,N]	2.31			
	26 VH [O,N]	2.31			
	38 VV [O,N]	1.65			
	38 VH [O,N]	1.65			

[a] Measurement site 1
[b] Measurement site 2

3.7 GHz. The CI, AB, CIF, and ABG models have unique path loss exponents, which come in at 5.74, 5.36, 5.67, and 5.49, respectively. Among the path loss exponents, the AB model offers a lower value. As we can see, the measured path loss-fitted LS models show almost the same behaviors for all the models and fit well the measured results.

Figure 7 shows the recorded path loss suited to the studied models with horn-to-horn antenna links at 28 GHz. We can see that the measured path loss fitted by the CI, CIF, and ABG models and the AB model match the measured results differently. The PLE of the CI, AB, CIF, and ABG models are respectively 4.52, 0, 5.53, and 5.26. Thus, at 28 GHz operating frequency, the AB model fits the measured results well. In Table 3, the statistical coefficients of the LS techniques are shown as determined using the campaigned dataset.

Table 4 shows the existing reported path loss exponents in the literature with their associated link specifications.

As we can see, the PLE in Table 3 is comparable to the PLE reported in Table 4 by other experimental studies. The PLE calculated from our measurement data ranges between 5.39 and 6.19 for each model. However, the value of PLE for the AB model is slightly higher, 10.26 at a 28 GHz link.

The free-space path loss of the CI and CIF models is fixed at 1 meter; as a result, the FSPL of these two models is constant in our study and the report studied by other researchers. However, the optimization procedure fixed the value of the FSPL of the AB and ABG models. Evidence from other studies suggests that the FSPL of ABG is less than those of the other three models. The value of the FSPL for the AB model reported in the existing literature is less than the CI and CIF model, according to the other studies. However, our study shows that the FSPL of the AB model is 44.96, 48.05, and 25.42 dB for, respectively, 3.7 GHz horizontal-to-horizontal link, 3.7 GHz horizontal-to-omnidirectional link, and 28 GHz horizontal-to-omnidirectional link. All these results are comparable for 28.00 dB for 28 GHz vertical-to-vertical link [21], 33.80 dB for 32 GHz vertical-to-vertical link [21], and 36.60 for 3.5 GHz for vertical-to-vertical link [22].

In our study, we find that $b = 0.0026$ and $\gamma = 2.45$. In the literature, however, the value of b is between -0.012 and 0.05, and the value of γ is between -4.80 and 2.81 [21], [22], [23], [26]. Therefore, the values we got for b and γ are like what has been reported in the literature. Consequently, the campaigned dataset is validated with the reported statistical coefficients.

V. CONCLUSION

This research examined LS path loss models at varying distances and frequencies in an indoor emergency stairwell, using data obtained with various antenna types and operating frequencies. In addition, we retrieved the PLE from the recorded dataset and the standard deviations of the four considered models. We validated the results by comparing them to other PLE studies. Each of the four models exhibits excellent agreement with the measured data. However, the AB model had a lower standard deviation than the other four models, which suggests that path loss variations are less likely to happen with the AB model. We have also noticed that the path loss does not change significantly in different antenna configurations, e.g., from horn to omnidirectional antenna; it does not vary significantly compared to the same type, e.g., from horn to horn antenna link. Comparing the measured data to previously reported data in the literature showed that the data was statistically valid.

TABLE 5. Meanings of the used symbols.

Symbol(s)	Meanings
α, β, γ	Statistical parameters of the ABG model
χ_{ABG}	Variations of received signal strength at the receiver side with ABG model
χ_{CIF}	Gaussian random variable with zero mean and a finite standard deviation
d	Three-dimensional Euclidean distance between the transmitter and receiver
n	Path loss exponent
χ_{CI}	Gaussian random variable with a zero mean and finite standard deviation
$\mathrm{FSPL}(f, d_0)$	Projected path loss at d_0 (in m) distance at f GHz
$\mathrm{P_{RAG}}$	Receiver antenna gain
$\mathrm{P_{RCL}}$	Total attenuation in the transmission cable at the receiver to the vector analyzer
$\mathrm{P_{RSL}}$	Received signal strength at the receiver side
$\mathrm{P_{TAG}}$	Transmitter antenna gain
$\mathrm{P_{TCL}}$	Total attenuation in the transmission cable at the transmitter to generator
$\mathrm{P_{TSL}}$	Transmitted signal strength level
$\mathrm{PL_{ABG}}$	Path loss as a function of the distance parameter d (m) and the frequency parameter f (GHz)
$\mathrm{PL_{CI}}$	Path loss in the CI path loss model as a function of distance d and frequency f
$\mathrm{PL_{CIF}}$	Path loss conditional on the distance parameters d and frequency f in the CIF model
$\mathrm{PL}(d)$	Path loss in decibels at a distance of d from the transmitter
$\mathrm{PL}\,(d_0)$	Path loss in the reference distance from transmitter d_0, and χ is a Gaussian random variable with a zero-mean and finite standard deviation

APPENDIX
LIST OF THE SYMBOLS

A list of the meaning of the used symbols are given in Table 5

REFERENCES

[1] M. F. Iskander and Z. Yun, "Propagation prediction models for wireless communication systems," *IEEE Trans. Microw. Theory Techn.*, vol. 50, no. 3, pp. 662–673, Mar. 2002, doi: 10.1109/22.989951.

[2] Y. Yu, Y. Liu, W.-J. Lu, and H.-B. Zhu, "Propagation model and channel simulator under indoor stair environment for machine-to-machine applications," in *Proc. Asia–Pacific Microw. Conf. (APMC)*, Nanjing, China, vol. 2, Dec. 2015, pp. 1–3, doi: 10.1109/apmc.2015.7413172.

[3] M.-S. Pan, C.-H. Tsai, and Y.-C. Tseng, "Emergency guiding and monitoring applications in indoor 3D environments by wireless sensor networks," *Int. J. Sensor Netw.*, vol. 1, nos. 1–2, pp. 2–10, Jan. 2006, doi: 10.1504/ijsnet.2006.010829.

[4] R. Deka, V. Mishra, I. Ahmed, S. Anees, and M. S. Alam, "On the performance and optimization of HAPS assisted dual-hop hybrid RF/FSO system," *IEEE Access*, vol. 10, pp. 80976–80988, 2022, doi: 10.1109/ACCESS.2022.3195930.

[5] G. Xu and Z. Song, "Performance analysis of a UAV-assisted RF/FSO relaying systems for Internet of Vehicles," *IEEE Internet Things J.*, vol. 9, no. 8, pp. 5730–5741, Apr. 2022, doi: 10.1109/JIOT.2021.3051211.

[6] L. Qu, G. Xu, Z. Zeng, N. Zhang, and Q. Zhang, "UAV-assisted RF/FSO relay system for space-air-ground integrated network: A performance analysis," *IEEE Trans. Wireless Commun.*, vol. 21, no. 8, pp. 6211–6225, Aug. 2022, doi: 10.1109/TWC.2022.3147823.

[7] J. Peng, X. He, C. Shi, J. Leng, F. Lin, F. Liu, H. Zhang, and W. Shi, "Investigation of graphene supported terahertz elliptical metamaterials," *Phys. E, Low-Dimensional Syst. Nanostruct.*, vol. 124, Oct. 2020, Art. no. 114309, doi: 10.1016/j.physe.2020.114309.

[8] A. I. Sulyman, A. Alwarafy, G. R. MacCartney, T. S. Rappaport, and A. Alsanie, "Directional radio propagation path loss models for millimeter-wave wireless networks in the 28-, 60-, and 73-GHz bands," *IEEE Trans. Wireless Commun.*, vol. 15, no. 10, pp. 6939–6947, Oct. 2016, doi: 10.1109/TWC.2016.2594067.

[9] L. Yu and L. B. White, "Optimum receiver design for broadband Doppler compensation in multipath/Doppler channels with rational orthogonal wavelet signaling," *IEEE Trans. Signal Process.*, vol. 55, no. 8, pp. 4091–4103, Aug. 2007, doi: 10.1109/TSP.2007.896028.

[10] J. Zhu, H. Wang, and W. Hong, "Large-scale fading characteristics of indoor channel at 45-GHz band," *IEEE Antennas Wireless Propag. Lett.*, vol. 14, pp. 735–738, 2015, doi: 10.1109/LAWP.2014.2377952.

[11] A. M. Al-Samman, T. A. Rahman, M. H. Azmi, and M. N. Hindia, "Large-scale path loss models and time dispersion in an outdoor line-of-sight environment for 5G wireless communications," *AEU-Int. J. Electron. Commun.*, vol. 70, no. 11, pp. 1515–1521, Nov. 2016, doi: 10.1016/j.aeue.2016.09.009.

[12] C. Phillips, D. Sicker, and D. Grunwald, "A survey of wireless path loss prediction and coverage mapping methods," *IEEE Commun. Surveys Tuts.*, vol. 15, no. 1, pp. 255–270, 1st Quart., 2013, doi: 10.1109/SURV.2012.022412.00172.

[13] A. Al-Saman, M. Mohamed, M. Cheffena, and A. Moldsvor, "Wideband channel characterization for 6G networks in industrial environments," *Sensors*, vol. 21, no. 6, p. 2015, 2021, doi: 10.3390/s21062015.

[14] S. Yong Lim, Z. Yun, J. M. Baker, N. Celik, H.-S. Youn, and M. F. Iskander, "Radio propagation in stairwell: Measurement and simulation results," in *Proc. IEEE Antennas Propag. Soc. Int. Symp.*, North Charleston, SC, USA, Jun. 2009, pp. 3239–3242, doi: 10.1109/APS.2009.5172260.

[15] S. Y. Lim, Z. Yun, J. M. Baker, N. Celik, H. S. Youn, and M. F. Iskander, "Propagation modeling and measurement for a multifloor stairwell," *IEEE Antennas Wireless Propag. Lett.*, vol. 8, pp. 583–586, 2009, doi: 10.1109/LAWP.2009.2021870.

[16] S. Yong Lim, Z. Yun, and M. F. Iskander, "Radio propagation measurements in multifloor indoor stairwells," in *Proc. IEEE Int. Conf. Wireless Inf. Technol. Syst.*, Honolulu, HI, USA, Sep. 2010, pp. 1–4, doi: 10.1109/ICWITS.2010.5611862.

[17] C. H. Teh and H. Chuah, "Propagation measurement in a multi-floor stairwell for model validation," in *Proc. 28th Int. Union Radio Sci. Gen. Assem.*, 2005, pp. 1–4, [Online]. Available: https://www.ursi.org/proceedings/procGA05/pdf/F03.5(0004).pdf

[18] O. A. Aziz and T. A. Rahman, "Investigation of path loss prediction in different multi-floor stairwells at 900 MHz and 1800 MHz," *Prog. Electromagn. Res. M*, vol. 39, pp. 27–39, 2014, doi: 10.2528/pierm14061904.

[19] V. A. Fono, L. Talbi, O. A. Safia, M. Nedil, and K. Hettak, "Deterministic modeling of indoor stairwells propagation channel," *IEEE Antennas Wireless Propag. Lett.*, vol. 19, no. 2, pp. 327–331, Feb. 2020, doi: 10.1109/LAWP.2019.2961641.

[20] Y. Yang, J. Sun, W. Zhang, C.-X. Wang, and X. Ge, "Ray tracing based 60 GHz channel clustering and analysis in staircase environment," in *Proc. IEEE Global Commun. Conf.*, Singapore, Dec. 2017, pp. 1–5, doi: 10.1109/glocom.2017.8254478.

[21] A. M. Al-Samman, T. A. Rahman, N. Hindia, and J. Nasir, "Path loss model for indoor emergency stairwell environment at millimeter wave band for 5G network," *Turkish J. Electr. Eng. Comput. Sci.*, vol. 26, no. 6, pp. 3024–3032, Nov. 2018, doi: 10.3906/elk-1710-248.

[22] A. Al-Saman, M. Mohamed, and M. Cheffena, "Radio propagation measurements in the indoor stairwell environment at 3.5 and 28 GHz for 5G wireless networks," *Int. J. Antennas Propag.*, vol. 2020, pp. 1–10, Dec. 2020, doi: 10.1155/2020/6634050.

[23] A. O. Aldhaibani, T. A. Rahman, and A. Alwarafy, "Radio-propagation measurements and modeling in indoor stairwells at millimeter-wave bands," *Phys. Commun.*, vol. 38, Feb. 2020, Art. no. 100955, doi: 10.1016/j.phycom.2019.100955.

[24] Y. Yu, Y. Liu, W.-J. Lu, and H.-B. Zhu, "Path loss model with antenna height dependency under indoor stair environment," *Int. J. Antennas Propag.*, vol. 2014, pp. 1–6, Jan. 2014, doi: 10.1155/2014/482615.

[25] S. Y. Lim, Z. Yun, and M. F. Iskander, "Radio propagation modeling in indoor stairwell: A K-means clustering approach," in *Proc. IEEE Int. Symp. Antennas Propag.*, Chicago, IL, USA, Jul. 2012, pp. 1–2, doi: 10.1109/aps.2012.6347999.

[26] S. Yong Lim, Z. Yun, and M. F. Iskander, "Propagation measurement and modeling for indoor stairwells at 2.4 and 5.8 GHz," *IEEE Trans. Antennas Propag.*, vol. 62, no. 9, pp. 4754–4761, Sep. 2014, doi: 10.1109/TAP.2014.2336258.

[27] Y. Shen, Y. Shao, L. Xi, H. Zhang, and J. Zhang, "Millimeter-wave propagation measurement and modeling in indoor corridor and stairwell at 26 and 38 GHz," *IEEE Access*, vol. 9, pp. 87792–87805, 2021, doi: 10.1109/ACCESS.2021.3081822.

[28] C. Zhang, J. Sun, Y. Liu, W. Zhang, and C.-X. Wang, "Channel characteristics analysis of 60 GHz wireless communications in staircase environments," in *Proc. IEEE/CIC Int. Conf. Commun. China*, Chongqing, China, Aug. 2020, pp. 7–12, doi: 10.1109/ICCCWORKSHOPS49972.2020.9209915.

[29] Y. Yu, J. Dong, A.-P. Ye, B. Yang, J. Liu, Y. Liu, W.-J. Lu, and H.-B. Zhu, "Effect of antenna height on propagation characteristics under indoor stair environment," in *Proc. 3rd Asia–Pacific Conf. Antennas Propag.*, Harbin, China, Jul. 2014, pp. 710–712, doi: 10.1109/APCAP.2014.6992595.

[30] N. Oyj. (Feb. 2023). *Nokia Wins New 10-Year 5G Deal With Antina in Singapore*. Accessed: Mar. 14, 2023. [Online]. Available: https://www.yahoo.com/now/nokia-wins-10-5g-deal-040000226.html

[31] (Dec. 2021). *5G: MAFAB, MTN Emerge Winners in Nigerias 3.5 GHz Spectrum Auction*. Accessed: Mar. 14, 2023. [Online]. Available: https://ncc.gov.ng/media-centre/news-headlines/1137-5g-mafab-mtn-emerge-winners-in-nigeria-s-3-5ghz-spectrum-auction

[32] (Nov. 2022). *Ericsson Report Highlights Potential Economic Benefits of 5G in Emerging Markets*. Accessed: Mar. 14, 2023. [Online]. Available: https://www.ericsson.com/en/press-releases/2022/11/ericsson-raceport-highlights-potential-economic-benefits-of-5g-in-emerging-markets

[33] S. Su-Hyun. (May 2021). *[News Focus] is 'Real 5G' Elusive Goal for Korea?* Accessed: Mar. 14, 2023. [Online]. Available: http://www.koreaherald.com/view.php?ud=20210530000162

[34] M. Khalily, S. Taheri, S. Payami, M. Ghoraishi, and R. Tafazolli, "Indoor wideband directional millimeter wave channel measurements and analysis at 26 GHz, 32 GHz, and 39 GHz," *Trans. Emerg. Telecommun. Technol.*, vol. 29, no. 10, p. e3311, Oct. 2018, doi: 10.1002/ett.3311.

[35] G. R. Maccartney, T. S. Rappaport, S. Sun, and S. Deng, "Indoor office wideband millimeter-wave propagation measurements and channel models at 28 and 73 GHz for ultra-dense 5G wireless networks," *IEEE Access*, vol. 3, pp. 2388–2424, 2015, doi: 10.1109/ACCESS.2015.2486778.

[36] C. R. Anderson and T. S. Rappaport, "In-building wideband partition loss measurements at 2.5 and 60 GHz," *IEEE Trans. Wireless Commun.*, vol. 3, no. 3, pp. 922–928, May 2004, doi: 10.1109/TWC.2004.826328.

[37] M. Bal, A. Marey, H. F. Ates, T. Baykas, and B. K. Gunturk, "Regression of large-scale path loss parameters using deep neural networks," *IEEE Antennas Wireless Propag. Lett.*, vol. 21, no. 8, pp. 1562–1566, Aug. 2022, doi: 10.1109/LAWP.2022.3174357.

[38] M. Abdus Samad and D.-Y. Choi, "Analysis and modeling of propagation in tunnel at 3.7 and 28 GHz," *Comput., Mater. Continua*, vol. 71, no. 2, pp. 3127–3143, 2022, doi: 10.32604/cmc.2022.023086.

[39] G. R. MacCartney, J. Zhang, S. Nie, and T. S. Rappaport, "Path loss models for 5G millimeter wave propagation channels in urban microcells," in *Proc. IEEE Global Commun. Conf. (GLOBECOM)*, Atlanta, GA, USA, Dec. 2013, pp. 3948–3953, doi: 10.1109/GLOCOM.2013.6831690.

MD. ABDUS SAMAD (Member, IEEE) received the Ph.D. degree in information and communication engineering from Chosun University, Gwangju, South Korea. He was an Assistant Professor with the Department of Electronics and Telecommunication Engineering, International Islamic University Chittagong, Chattogram, Bangladesh, from 2013 to 2017. He has been an Assistant Professor with the Department of Information and Communication Engineering, Yeungnam University, South Korea. His research interests include signal processing, antenna design, electromagnetic wave propagation, applications of artificial neural networks, deep learning, and millimeter-wave propagation by interference or atmospheric causes for 5G and beyond wireless networks. He received the prestigious Korean Government Scholarship (GKS) for his Ph.D. studies.

DONG-YOU CHOI (Senior Member, IEEE) received the B.S., M.S., and Ph.D. degrees from the Department of Electronics Engineering, Chosun University, Gwangju, South Korea, in 1999, 2001, and 2004, respectively. Since 2006, he has been a Professor with the Department of Information and Communication Engineering, Chosun University. His research interests include rain attenuation, antenna design, wave propagation, and microwave and satellite communication. He is a member of KEES, IEEK, and KICS.

HYUNGSEOP SON received the B.S. degree from Yeungnam University, Gyeongsan-si, South Korea, in 2023, where he is currently pursuing the M.S. degree with the Department of Information and Communication Engineering. His research interest includes advanced communication systems.

KWONHUE CHOI (Senior Member, IEEE) received the B.S., M.S., and Ph.D. degrees in electronic and electrical engineering from the Pohang University of Science and Technology, Pohang, South Korea, in 1994, 1996, and 2000, respectively. From 2000 to 2003, he was with the Electronics and Telecommunications Research Institute, Daejeon, South Korea, as a Senior Research Staff Member. In 2003, he joined the Department of Information and Communication Engineering, Yeungnam University, Gyeongsan-si, South Korea, where he is currently a Professor. He has authored a textbook titled *Problem-Based Learning in Communication Systems Using MATLAB and Simulink* (Wiley, 2016). His research interests include signal design for communication systems, multiple access schemes, diversity schemes for wireless fading channels, multiple antenna systems, and in-band full-duplex systems.